J Biol Inorg Chem (2004) 9: 335–344
DOI 10.1007/s00775-004-0534-3

ORIGINAL ARTICLE

Hemanta Baruah · Ulrich Bierbach

Biophysical characterization and molecular modeling of the coordinative-intercalative DNA monoadduct of a platinum-acridinylthiourea agent in a site-specifically modified dodecamer

Received: 8 December 2003 / Accepted: 23 February 2004 / Published online: 16 March 2004

Abstract The guanine-*N7* monoadduct of [Pt(en)Cl(ACRAMTU)]$(NO_3)_2$ (PT-ACRAMTU; en = ethane-1,2-diamine, ACRAMTU = 1-[2-(acridin-9-ylamino) ethyl]-1,3-dimethylthiourea), a dual metalating/intercalating cytotoxic agent, was generated in a double-stranded dodecamer, d(CCTCTCG*TCTCC/GGAG ACGAGAGG) (**III***), and isolated by preparative reverse-phase high-performance liquid chromatography (HPLC). The adduct was characterized using matrix-assisted laser desorption/ionization time-of-flight mass spectrometry (MALDI-TOF MS), circular-dichroism spectropolarimetry (CD), UV-melting curves, and NMR spectroscopy. In addition, a molecular mechanics/restrained molecular dynamics (MM/rMD) study was performed for this adduct using the AMBER force field. Monoadduction of the sequence leads to a pronounced increase in melting temperature, $\Delta T_m = T_m$(**III***)$-T_m$(**III**) = 9.7 °C. Because there is complete enthalpy–entropy compensation, binding occurs without noticeable thermodynamic destabilization. This feature and the CD (induced-ligand circular dichroism) and NMR (upfield shifts of aromatic acridine proton signals) data are indicative of a unique, nondenaturing dual-binding mode that involves partial intercalation of the acridine chromophore. An energy-minimized AMBER model of **III*** demonstrates that platination of G7-*N7* of guanine in the major groove and partial insertion of the acridine moiety into the C6G19/G7C18 base step on the 5′ face of the modified purine base is feasible and supportive of the experimental results. Differences in the biophysical properties between **III*** and duplexes containing adducts of the clinical-drug cisplatin are outlined, and possible biological consequences are discussed.

Keywords Conformation · Conjugate · DNA · Intercalation · Platinum

Abbreviations *ACRAMTU* 1-[2-(acridin-9-ylamino)ethyl]-1,3-dimethylthiourea · *dGuo* 2′-deoxyguanosine · *dGuo** [Pt(en)(ACRAMTU-*S*)(dGuo-*N7*)]$^{3+}$ · *en* ethane-1,2-diamine · *ICD* Induced circular dichroism · *MALDI-TOF MS* Matrix-assisted laser desorption ionization time-of-flight mass spectrometry · *MM* Molecular mechanics · *PIPES* 1,4-piperazinediethanesulfonic acid · *PT-ACRAMTU* [Pt(en)Cl(ACRAMTU)]$(NO_3)_2$ · *rMD* Restrained molecular dynamics

Introduction

The vast majority of anticancer drugs that interact directly with DNA are covalent cross-linkers or topoisomerase-directed intercalators [1]. In following our interest in clinically useful DNA-targeted pharmacophores, we have designed novel hybrid agents that combine the classical DNA-binding modes of platination and intercalation [2]. The rationale behind the design of such conjugates is that they might form new types of adducts that cause structural effects in DNA not observed for their individual components. The differential recognition of a new type of lesion by DNA-processing-and-binding enzymes and proteins would ultimately lead to a unique spectrum of biological activity.

PT-ACRAMTU (ACRAMTU = 1-[2-(acridin-9-ylamino)ethyl]-1,3-dimethylthiourea, acridinium cation; Fig. 1) is a new potent cytotoxic agent that binds to DNA through a combination of monofunctional metalation of nucleobase nitrogen and intercalation of the acridine chromophore, linked to the thiourea nonleaving

Electronic Supplementary Material Supplementary material is available in the online version of this article at http://dx.doi.org/10.1007/s00775-004-0534-3

H. Baruah · U. Bierbach (✉)
Department of Chemistry,
Wake Forest University,
P.O. Box 7486 Reynolda Station,
Winston-Salem, NC 27109, USA
E-mail: bierbau@wfu.edu
Tel.: +1-336-7583507
Fax: +1-336-7584656

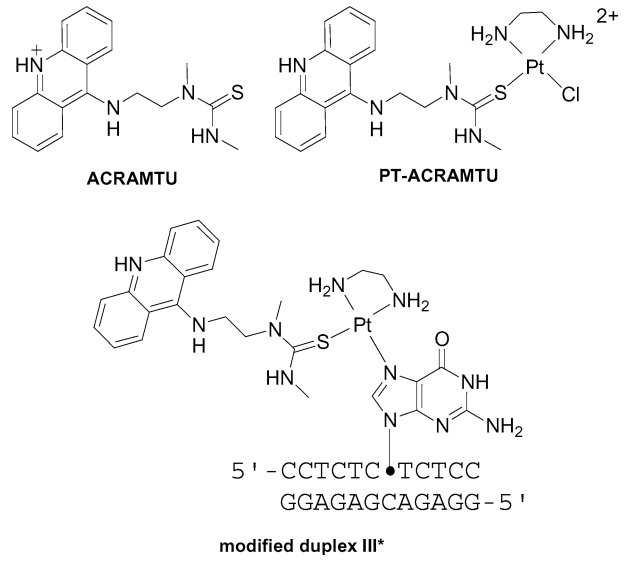

Fig. 1 Structures of the acridinylthiourea (ACRAMTU), its platinum conjugate (PT-ACRAMTU), and the modified double-stranded dodecamer (**III***)

group, into the DNA base stack [3]. The formation of a single purine–metal coordinative bond by these agents is in contrast to the mechanism of platinum-based chemotherapies currently in clinical use, such as *cis*-diamminedichloroplatinum(II) (cisplatin, *cis*-$[PtCl_2(NH_3)_2]$), which induce purine–purine cross-links [4]. The concept of DNA-targeted platinum complexes, pioneered by Bowler and Lippard [5], has inspired the design of numerous conjugates that contain the classical *cis*-dichloroplatinum(II) unit flexibly tethered to a suitably modified intercalator (for some recent developments see [6, 7, 8]). In contrast, few conjugates containing monochloroplatinum(II) groups have been described [9]. While the DNA-sequence specificity of these species has been studied in detail [10, 11], no attempts have been made, to the best of our knowledge, to characterize site-specific DNA adducts of these compounds.

In double-stranded DNA, PT-ACRAMTU targets guanine and adenine bases. The most abundant (approximately 80%) drug-modified DNA fragment detected in enzymatic digests of native DNA treatedwith PT-ACRAMTU was the mononucleoside adduct,[Pt(en)(ACRAMTU-*S*)(dGuo-*N7*)]$^{3+}$ (dGuo*; dGuo = 2′-deoxyguanosine, the asterisk indicates the fragment [Pt(en)(ACRAMTU-*S*)]$^{3+}$) [12]. dGuo* forms when the chloro leaving group in PT-ACRAMTU is replaced with endocyclic-nitrogen N7 of guanine, which is located in the major groove of the biopolymer. Multinuclear-NMR spectroscopy, high-performance liquid chromatography (HPLC), electrospray (tandem) mass spectrometry [12], and more recently, single-crystal X-ray diffraction (unpublished results), have been used to determine the structure and reactivity of dGuo*. In 20% of the adducts, which were identified as the modified dinucleotide fragments [5′-GpA*]$^{2+}$ and [5′-TpA*]$^{2+}$, PT-ACRAMTU binds to adenine, most likely at the N3 position [12]. The latter two damage sites, which are unprecedented in platinum antitumor chemistry, reflect the sequence specificity of ACRAMTU, suggesting that in these adducts the intercalating moiety, rather than the metal, dictates the sites of platination.

The unique adduct profile of PT-ACRAMTU demonstrates that platinum and acridine are functionally interdependent: in 20% of the adducts, divalent platinum, which has a naturally high affinity for guanine-*N7*, is "hijacked" to the preferred intercalation sites of ACRAMTU, where it binds to adenine. On the other hand, the planar chromophore is anchored into the major groove in guanine-*N7* adducts of the conjugate, which is in contrast to free ACRAMTU: this 9-aminoacridine derivative has been demonstrated to selectively intercalate into B-form DNA from the minor groove [13]. In the present study, we have synthesized a double-stranded model oligonucleotide containing the guanine-*N7* monoadduct of PT-ACRAMTU and characterized the modified duplex using various physical methods, including MALDI-TOF mass spectrometry, circular-dichroism spectropolarimetry, thermal melting curves, NMR spectroscopy, and molecular-modeling techniques. The combined data provide strong evidence for a unique hybrid coordinative-intercalative binding mode, whose structural impact on DNA appears to be different from that of bifunctional cisplatin-type damage.

Materials and methods

Starting materials

The synthesis and characterization of ACRAMTU and its platinum conjugate (PT-ACRAMTU) were published earlier [2]. Both drugs were used in their nitrate salt forms. Buffers were made from biochemical-grade chemicals (Fisher/Acros) using 0.22 μm-filtered DNase/RNase-free water obtained from a Milli-Q A10 synthesis water-purification system. All experiments were carried out in a buffer of pH 7.0 containing 10 mM PIPES (1,4-piperazinediethanesulfonic acid) and 150 mM NaCl. HPLC-grade solvents were used for all chromatographic separations. All other chemicals and reagents were purchased from common vendors and used without further purification. The oligodeoxyribonucleotides 5′-CCTCTCGTCTCC-3′ (sequence **I**) and 5′-GGAGACGAGAGG-3′ (sequence **II**) were purchased from Integrated DNA Technologies Inc. (Coralville, IA, USA). The sequences were synthesized using phosphoramidite chemistry and desalted by the vendor. The DNA strands were quantified by UV-visible spectroscopy using the molar-extinction coefficients $\epsilon_{I,260} = 94{,}300$ l/cm mol and $\epsilon_{II,260} = 131{,}700$ l/cm mol provided by the vendor. Stock solutions of the DNA-drug adducts were kept at −20 °C for long-term storage.

Platination and purification of the modified top strand (**I***)

Sequence **I** (2.9 μmol) was incubated with 1.1 equivalents (3.2 μmol) of PT-ACRAMTU in 2 ml of water (pH 6.0) at 37 °C for 5 days in the dark. The reaction was followed by HPLC (LaChrom Hitachi D-7000 system equipped with an L-7420 UV-visible variable-wavelength detector). A semipreparative reverse-phase column (250×10 mm; Hamilton PRP-1) was used for both moni-

toring the progress of the reaction and product isolation. Chromatograms were recorded at monitoring wavelengths of 254 and 413 nm for analytical purposes and at 285 nm during adduct collection. The separation of the reaction mixture was carried out under the following conditions: mobile phase—solvent A = 100 mM ammonium acetate, pH 7.0; solvent B = 100% acetonitrile; gradients—(1) 90% A/10% B → 60% A/40% B over a period of 40 min at a flow rate of 3 ml/min or (2) 95% A/5% B → 92% A/8% B for 6 min followed by isocratic flow at 92% A/8% B from 6 min to 18 min; flow rate 3 ml/min. Adduct **I*** was collected, lyophilized, redissolved in 1 ml of water, and desalted by exhaustive dialysis against deionized water (Spectrum Spectro/Por 1 ml DispoDialyzer unit, 500 Da molecular-weight cut-off). A 30-μg lyophilized sample of **I*** was analyzed by MALDI-TOF mass spectrometry.

Duplex preparations

The unmodified and modified duplexes **III** and **III*** were generated by mixing suitable aliquots of buffered solutions of **II** with **I** and **I***, respectively. To ensure complete double-strand formation, the samples were annealed by heating at 75 °C for 2 min followed by slow cooling to room temperature. Concentrations of the strands were determined spectrophotometrically using molar-extinction coefficients ϵ_{260} for the DNA (see above) and $\epsilon_{420} = 6.44\times10^3$ l/cm mol for DNA-bound acridine [3]. A duplex formation of 1:1 was established using continuous-variation titrations (Job plot analysis [14]). Noncovalent complexes of **III** and ACRAMTU at various drug-to-DNA ratios were generated by titrating aliquots of a concentrated stock solution of ACRAMTU ($\epsilon_{413} = 9.45\times10^3$ l/cm mol) to the DNA, maintaining a constant concentration of duplex in all cases. Samples were thoroughly mixed and equilibrated for 2 min before measurements. An annealed sample of **III*** was analyzed using MALDI-TOF mass spectrometry. The following numbering scheme was used for **III***:

5′-C(1)C(2)T(3)C(4)T(5)C(6)G*(7)T(8)C(9)T(10)C(11)C(12)-3′
3′-G(24)G(23)A(22)G(21)A(20)G(19)C(18)A(17)G(16)A(15)G(14)G(13)-5′

MALDI-TOF mass spectrometry

MALDI-TOF mass spectra of desalted samples of **I*** and **III*** were recorded on a Voyager DE instrument (Applied Biosystems Inc., Foster City, CA, USA) by HT-Laboratories (San Diego, CA, USA).

Circular-dichroism spectropolarimetry

CD experiments were performed on an AVIV Model 215 spectrophotometer equipped with a thermoelectrically controlled cell holder. Quartz cells with 1 cm path length were used for all experiments. Before data collection, samples were annealed by slow cooling from 75 °C to room temperature. The duplex-DNA concentrations were 3.2 μM and 83 μM for CD spectra recorded in the UV (220–320 nm) and UV-visible (320–600 nm) regions, respectively. Isothermal CD spectra at 25 °C were recorded in 1-nm increments with an averaging time of 1 s.

Optical studies of thermal denaturation

The melting profiles were recorded on an HP 8453 diode array spectrophotometer equipped with a Peltier temperature-controlled cell-holder unit and an external temperature probe. Quartz cells with 1 cm path length were used in all experiments. Duplex concentrations were maintained at 2.3 μM. Absorbance as a function of temperature was measured at 260 nm. The temperature was raised in 1 °C increments, and the stirred samples were allowed to equilibrate for 2 min at each temperature setting. Absorbance data were collected in the temperature range 25–80 °C and fitted to the baseline-corrected two-state helix-coil transition model [15] (Eq. 1). Melting temperatures (T_m) and van't Hoff transition enthalpies (ΔH_{vH}) were extracted directly from the curve fits. Additional thermodynamic properties were calculated using Eqs. 2 and 3. Errors in the calculated data were estimated from experimental standard deviations. Thermal melting experiments for each duplex were performed in triplicate.

$$y = (m_1T + b_1) + (m_2T + b_2) \times \frac{e^{-\frac{\Delta H_{vH}}{RT} + \frac{\Delta H_{vH}}{RT_m}}}{1+e^{-\frac{\Delta H_{vH}}{RT} + \frac{\Delta H_{vH}}{RT_m}}} \quad (1)$$

(m_1, m_2, b_1, and b_2 are the slopes and y-intercepts of the lower and upper baselines, respectively)

$$\Delta S_{vH} = \Delta H_{vH}/T_m[\text{cal/mol K}] \quad (2)$$

$$\Delta G_{vH,25} = \Delta H_{vH} - (298.15)\Delta H_{vH}/T_m[\text{kcal/mol}] \quad (3)$$

Analysis of the melting transitions was carried out using the custom-defined nonlinear fitting option of Microcal Origin 6.0 (OriginLab Corp., Northampton, MA, USA).

NMR spectroscopy

Duplex **III*** was dissolved in 300 μl of buffer (10 mM PIPES, 150 mM NaCl, pH 7.0), lyophilized to dryness, and re-lyophilized twice using 99.96% D_2O. An NMR sample was made by dissolving the adduct in 300 μl of 99.996% D_2O to yield a concentration of approximately 1 mM of double-stranded oligonucleotide. A special NMR microtube (Shigemi Inc., Allison Park, PA, USA) was used for data collection. NMR data acquisition and processing: ^{1}H NMR spectra were acquired at 500 MHz on a Bruker DRX-500 spectrometer equipped with a 5-mm inverse 3-channel Z-gradient TBI probe and a variable-temperature unit with a total of 64 k data points, 256 transients, and a recycle delay of 1 s. An exponential window function with a line broadening of 2 Hz was used to apodize the time-domain data before Fourier transformation. ^{1}H NMR spectra of PT-ACRAMTU were taken in D_2O. All spectra were acquired at 25 °C with spectral widths of 5,000 Hz. Chemical shifts were referenced to the HDO peak, which was calibrated against external 3-(trimethylsilyl)-1-propanesulfonic acid sodium salt (DSS). Data were processed with Felix 2000 (Molecular Simulations Inc., San Diego, CA) installed on a Silicon Graphics O2 workstation.

Molecular modeling of the platinated duplex (**III***)

Calculations were performed using the program Discover, interfaced with InsightII (release 2000, Molecular Simulations Inc., San Diego, CA, USA) for visualization and analytical purposes. The AMBER forcefield was used in all molecular-mechanics calculations. Coordinates for PT-ACRAMTU bound to guanine were adopted from the crystal structure of the PT-ACRAMTU-guanosine adduct (dGuo*). Gasteiger-Hückel partial charges for ACRAMTU were adopted from a previous study [13]. The +2 charge on the platinum atom was distributed to the neighboring atoms according to a published scheme [16]. Ad-hoc force constants, bond lengths, angles, and torsionals, partly based on existing AMBER parameters [17, 18, 19], were optimized to accurately reproduce key structural features of the PT-ACRAMTU-guanosine adduct. (Newly introduced atom types and parameters can be found in Electronic Supplementary Material.) The B-form duplex of the unmodified sequence (**III**) was built with the Biopolymer module in InsightII.

Duplex **III*** was generated by attaching the [Pt(en)(ACRAMTU-*S*)]$^{3+}$ fragment to the N7 position of G7 in the major groove with the acridine chromophore inserted into the CG/CG base step, i.e., on the 5′ face of the platinated nucleobase. Sodium counter ions were placed at the O-P-O bisector of

each phosphodiester linkage to compensate the negative charge of the DNA backbone, and solvent was simulated with a distance-dependent dielectric ($\epsilon = 4r_{ij}$). A cut-off of 25 Å was used for nonbonded interactions with a switching distance of 1.5 Å. Coulombic and 1-4 nonbonded interactions were scaled by a factor of 0.5. For molecular-dynamics calculations, a flat-bottomed potential was applied with an energy penalty of 100 kcal/mol Å^2. Inside the restraint boundaries, no energy penalty was applied. Restraints were introduced between sodium ions and nearby phosphorus atoms (10 kcal/mol Å^2) and for Watson-Crick hydrogen bonds (100 kcal/mol Å^2). The starting structure was subjected to 10,000 iterations of steepest descent (delta rms = 1 kcal/mol Å) followed by conjugate gradient minimization until a derivative of less than 0.1 kcal/mol Å was achieved. The pre-minimized structure was then subjected to an MM/rMD protocol consisting of a heating phase of 10 ps from 0 to 150 K followed by 100 ps of dynamics at 150 K using a step size of 1 fs with all restraints "on". Along the dynamics trajectory, snapshots of the adduct were saved every 10 ps, which resulted in ten high-energy structures. Each of the structures was initially minimized with restraints "on" and finally with all restraints "off" to a final maximum derivative of 0.001 kcal/mol Å. An average structure was calculated using the program Analysis/InsightII. Helical parameters were analyzed with NAMOT (version 2.1; Carter G, Tung C-S; Los Alamos National Laboratory).

Results and discussion

Design and modification of the duplex

Previous DNA-unwinding experiments [3] using negatively supercoiled plasmid showed that covalently bound PT-ACRAMTU untwists the right-handed DNA helix by 21°/adduct, indicative of a dual-binding mode that involves (partial) intercalation of the planar chromophore into the DNA base stack. Acridines preferentially intercalate into 5′-pyrimidine/purine-3′ sequences, and ACRAMTU shows a high dual affinity for the dinucleotide steps 5′-TA-3′ and 5′-CG-3′ [13]. Transcription-inhibition assays reveal that the covalent DNA modifications by PT-ACRAMTU occur at the 3′ purine bases of these base steps (unpublished data). Apparently, ACRAMTU retains its sequence specificity as a carrier group in the corresponding conjugate causing damage in sequences previously unknown for clinical platinum drugs. (For instance, cisplatin produces interstrand cross-links at 5′-GC/GC but not at 5′-CG/CG [20].) Thus, a mechanism of DNA binding is predicted that involves platination of nucleophilic nucleobase nitrogen at the intercalation site of the acridine moiety. With this in mind, we have chosen a dodecamer sequence, d(CCTCTCGTCTCC)·d(GGAGACGAGAGG), containing a central 5′-CG/CG base step and a single guanine base in the top strand (note that this allows intercalation of the acridine unit on the 5′ face of the platinated base). The length and GC-content of the sequence and the thermal stability of the resulting duplex proved to be ideal for the biophysical and spectroscopic studies described. A similar sequence, in which C6 was substituted with G6, has been used in X-ray-crystallographic [21] and NMR-solution [22] studies of the 1,2 intrastrand d(GpG-*N7*,*N7*) cross-link formed by cisplatin, allowing a comparative analysis of the DNA structural impacts of the two drugs.

Modification of the top strand (**I**) with the monoadduct of PT-ACRAMTU yielded **I***, which was isolated and purified by preparative HPLC (Scheme 1, see Materials and methods section for details). The HPLC profiles showed the formation of one major adduct (>90%) that results from selective platination of G7-*N7*, as predicted from analogous reactions of the platinum conjugate with dGuo and native DNA [12]. MALDI-TOF MS analysis of **I*** (Fig. 2) confirmed the formation of a strong coordinative bond between platinum and the oligonucleotide. In spectra recorded in negative-ion mode, two major peaks are observed at m/z 4084 and m/z 2042 corresponding to the monoanionic and dianionic protonated forms of the modified strand, $[\mathbf{I}^* + 7H]^-$ and $[\mathbf{I}^* + 6H]^{2-}$. Sequence **I*** was hybridized with the bottom strand (**II**) to generate the desired duplex, **III***. Loss of ACRAMTU was not observed. Under the denaturing conditions of MALDI-TOF MS (not shown), duplex **III*** dissociates into **I*** ($[\mathbf{I}^* + 7H]^-$, m/z 4084) and **II** ($[\mathbf{II} + 10H]^-$, m/z 3783) indicating that the monoadduct remains intact during the annealing process ($T \approx 75$ °C) and does not undergo secondary reactions, such as cross-link formation promoted by the loss of ACRAMTU. ^{1}H NMR spectra (see below) of **III*** taken over a period of 2 weeks were practically unchanged, which confirmed the stability of the adduct.

Circular dichroism (CD)

CD spectropolarimetry has been used extensively to study the conformation of drug-modified nucleic acids. These include covalent mono- and bifunctional adducts formed by platinum anticancer agents [23] as well as noncovalent acridine–DNA complexes [24, 25, 26]. The two informative spectral regions are the DNA region where the nucleobases absorb ($\lambda < 300$ nm) and the ligand region ($\lambda > 300$ nm), which contains characteristic bands originating from π-π^* transitions within the planar 9-aminoacridine chromophore [27]. CD spectra were recorded for both the unmodified and modified duplexes

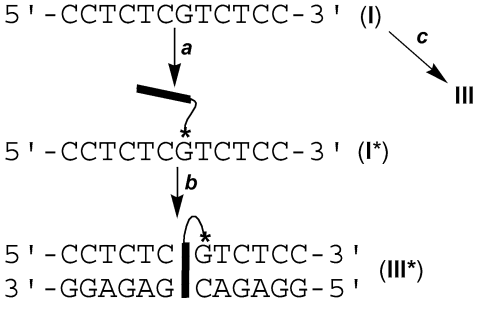

Scheme 1 Formation of platinum-modified and unmodified duplexes under the following conditions: *a* PT-ACRAMTU, 37 °C, pH 6.0, 5 days, HPLC purification, desalting; *b*, *c* mixing with bottom strand (**II**), annealing (Job plot analysis)

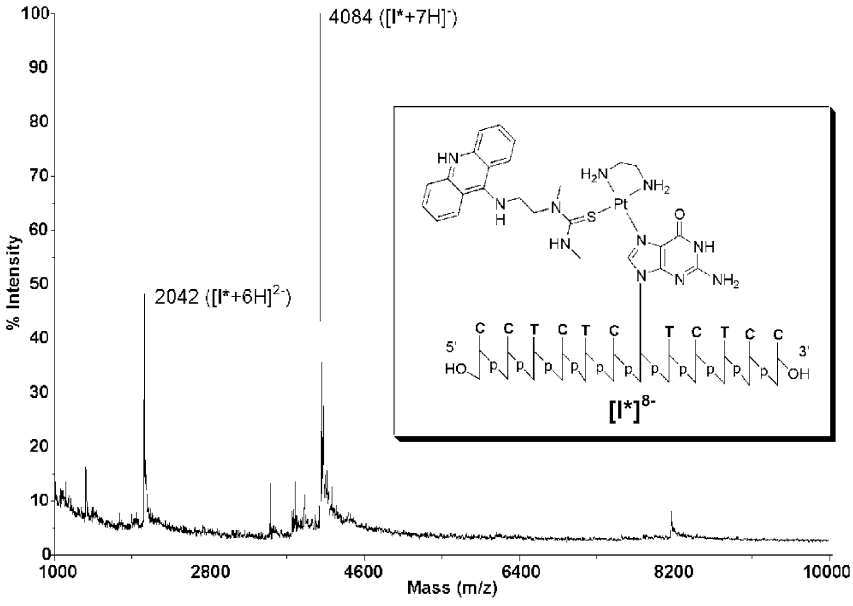

Fig. 2 Negative-ion MALDI-TOF mass spectrum and structure (*inset*) of the modified sequence **I***. The 8– charge of the adduct at physiological pH results from 11 negatively charged phosphates and the 3+ charge of the platinum-acridine fragment, [Pt(en) ACRAMTU]$^{3+}$

III and **III***, as well as for noncovalent complexes of **III** and ACRAMTU at varying ligand-to-duplex stoichiometries. (**III** contains five high-affinity intercalation sites of ACRAMTU, four 5′-GA/TC and one 5′-CG/CG [13].) Duplexes containing reversibly bound ACRAMTU were included in this study to examine differences in the intercalation modes of the simple intercalator and its platinum conjugate.

The results for the covalent and noncovalent complexes are shown in Fig. 3. The CD signal in the DNA region (Fig. 3a) for the unmodified sequence **III** shows a negative band at 240 nm and a positive band at 278 nm, the characteristic pattern expected for a right-handed, B-type duplex [28]. Upon addition of one equivalent of ACRAMTU to **III**, a pronounced decrease in the intensity, but no shifts, of the two bands is observed. Titration of additional ACRAMTU to the DNA (without changing the concentration of duplex) resulted in further decrease of the signal amplitudes (not shown). In contrast, CD spectra of **III*** containing a single drug adduct show a distinct shift of the negative and positive bands by 2 and 4 nm to longer wavelengths compared to **III**. The red-shift is accompanied by a decrease in intensity of the negative band and an increase in intensity of the positive band. These results suggest that the conformational changes in double-stranded DNA caused by ACRAMTU and PT-ACRAMTU are distinctly different, assuming that the circular dichroism in

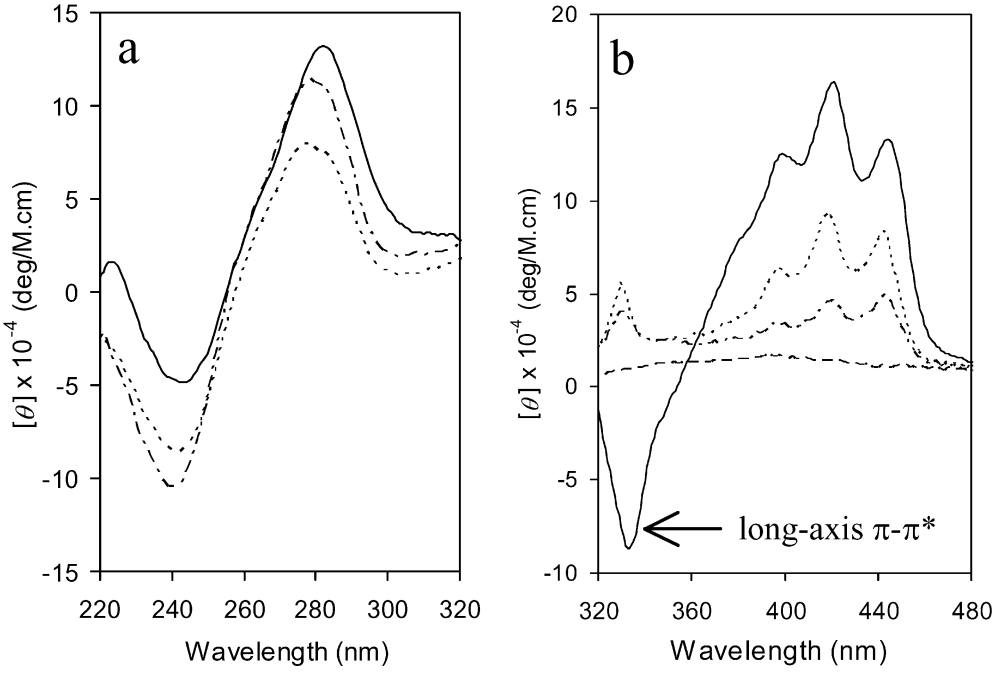

Fig. 3a, b CD spectra recorded at 25 °C of the unmodified and drug-modified dodecamers. **a** Signals in the DNA region for **III** (*dashed-dotted trace*), **III**·ACRAMTU (*short-dashed trace*), and **III*** (*solid trace*). **b** Signals in the ligand region for PT-ACRAMTU (*long-dashed trace*), **III**·ACRAMTU (*short-dashed trace*), **III**·5ACRAMTU (*dashed-dotted trace*), and **III*** (*solid trace*). Duplex concentrations in **a** and **b** were 3.2 μM and 83 μM, respectively (10 mM PIPES, 150 mM NaCl, pH 7.0)

the range 220–320 nm is dominated by the nucleobases. ACRAMTU also absorbs in this region (9-aminoacridine chromophores show weak transitions around 280 nm [27]), and some contribution from induced circular dichroism (ICD) originating from an intrinsically achiral ligand in a chiral environment cannot be fully excluded. For both the reversible and irreversible DNA binders, the duplexes appear to retain overall B-form parameters, and the observed spectral changes most likely reflect local perturbation of the helices at the adduct sites (a pronounced *blue-shift* of ~20 nm of the long-wavelength CD band, for instance, would have been expected for a B → A DNA conformational change [28]).

The ICD spectra in the 320–460 nm region, where the 9-aminoacridine chromophore absorbs, proved to be more informative (Fig. 3b). While the intensity of the bands centered around 330 and 420 nm is characteristic of intercalators [24], the signal signs give important clues about the binding geometry of the planar chromophore with respect to the sandwiching base pairs. The ICD band at 420 nm, which mimics the absorption spectrum of the chromophore, including its vibrational substructure, has a positive sign for duplexes modified both with ACRAMTU and PT-ACRAMTU. The site-specific covalent monoadduct of the platinum conjugate (**III***) gives the most intense ICD, followed by the reversible complexes **III**·ACRAMTU and **III**·5ACRAMTU. A decrease in intensity of the 420-nm ICD and a noticeable red-shift, accompanied by a change in the shape of the band is observed upon titration of multiple equivalents of ACRAMTU to duplex **III**. This observation can be explained with (1) increased chromophore–chromophore (exciton) interactions between stacked ligands at high ligand-to-duplex ratios and (2) heterogeneity of the ligand orientations relative to the base pairs [24, 27]. A distinct difference between the ICD spectra of the non-covalently modified duplexes and **III*** in the 330-nm region proves to be characteristic: the band is positive for ACRAMTU but negative for PT-ACRAMTU. Previous studies have assigned the two π-π^* transitions at 330 and 420 nm to electronic transitions polarized along the long and short axis of the 9-aminoacridine chromophore [27]. In ICD spectra of simple 9-aminoacridine, positive bands are observed for both transitions, which is usually discussed as evidence that the long axis of the chromophore is oriented *parallel* to the Watson-Crick hydrogen bonds [25]. The CD spectra in Fig. 3b suggest that ACRAMTU adopts this geometry; a previous detailed NMR/molecular-modeling study [13] also supports this. In contrast, the negative sign for the long-axis transition observed for platinum-tethered ACRAMTU in **III*** is highly suggestive of a geometry in which the chromophore is twisted away from the parallel orientation, resulting in a more perpendicular penetration of the duplex with respect to one or both of the adjacent base pairs [29]. A possible explanation is that intercalation of acridine in adducts of the platinum conjugate may be restricted due to the nature of the covalent linkage; this is supported by the modeling data (see below). A similar effect has been observed for bisacridines, for which steric factors allowed only partial intercalation of the chromophores [25].

NMR spectroscopy

Further evidence for intercalation of the acridine chromophore in **III*** was found in the ^{1}H NMR spectra of this adduct. The downfield region in spectra of **III*** (Fig. 4) showed multiple broad signals in the 6.4–7.1 ppm region where non-exchangeable protons of deoxyribonucleotides are usually not observed. The resonances were identified as the aromatic-ring protons, H1–H8, of the acridine chromophore based on inter-proton connectivities established for the signals in ^{1}H–^{1}H correlated spectra (not shown). These signals appear considerably upfield of those observed for free PT-ACRAMTU due to the shielding ring-current effect of the sandwiching nucleobases surrounding the chromophore, which is commonly considered evidence for an intercalative binding mode [30]. Upfield shifts of similar magnitude ($\Delta\delta$ 0.4–1 ppm) have been reported previously for double-stranded hexamers and octamers containing ACRAMTU [13]. The fact that the aromatic acridine protons in **III*** appear to no longer be pairwise equivalents supports the proposed asymmetric-intercalation mode. Five signals have been identified accounting for at least six protons (the signal at δ 7.06 integrates to two protons, and the signal at δ 7.71 could not be integrated due to signal overlap). The quality of the NMR data sets, which was limited due to the low sample concentration and severe spectral overlap, did not permit further assignment of the individual spin systems for H1-H4 and H5-H8, which, along with the shielding criteria, might have given additional information about the exact geometry of intercalation.

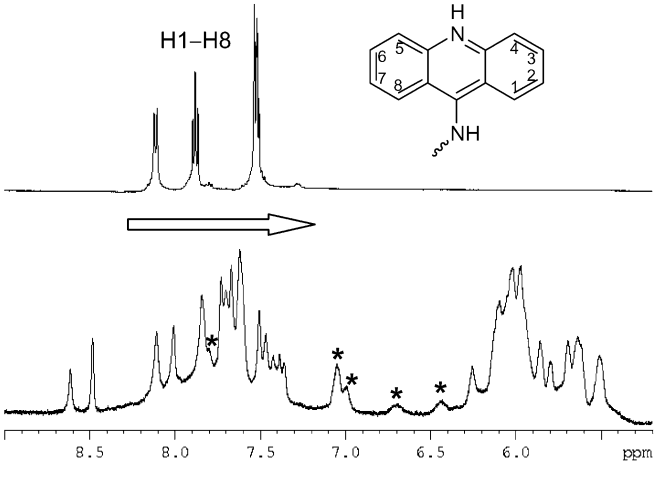

Fig. 4 ^{1}H NMR spectra (500 MHz, 25 °C, D_2O) of PT-ACRAMTU (*top*) and duplex **III*** (*bottom*). The *asterisks* denote the upfield-shifted signals of the aromatic acridine protons

Thermal melting studies

Changes in the thermodynamic stability of double-stranded DNA are thought to play an important role in the recognition and processing of biopolymers modified with covalent and noncovalent drug adducts. The thermal melting behavior of the modified DNA, usually monitored by differential-scanning calorimetry or UV-absorption spectrophotometry, can be used to extract thermodynamic parameters and gain insight into the type of chemical modification of the host duplex. We have recorded the UV–melting profiles of sequences **III**, **III**·ACRAMTU, **III**·3ACRAMTU, and **III*** (Fig. 5) and analyzed their shapes to estimate thermodynamic data of duplex formation (summarized in Table 1). Under the chosen experimental conditions ($c_{DNA} = 2.3$ μM, 150 mM NaCl), the unmodified sequence **III** was found to melt at 52.8 °C; this agrees well with the theoretical value of 52(±2) °C calculated using SantaLucia's nearest-neighbor model [31]. Titration of one and three equivalents of ACRAMTU to the duplex causes moderate increases in melting temperature (ΔT_m) of 1.7 and 1.9 °C, respectively (Fig. 5a). A similar small effect has been observed for this intercalator in poly(dA-dT)$_2$, modified at a drug-to-base pair ratio of 0.2, which had a ΔT_m of 1.3 °C [3]. A more dramatic change in melting temperature, $\Delta T_m = 9.7$ °C, is observed for the covalent adduct **III*** (Fig. 5b). This is unexpected, since monoadducts of platinum (as well as the 1,2 *intra*strand cross-link) usually lower the melting point of the host duplex [32]. It can be concluded that in the conjugate, the two binding modes, monofunctional platination and intercalation, act synergistically rather than additively.

Analysis of the van't Hoff parameters, ΔH_{vH}, ΔS_{vH}, and $\Delta G_{vH(25)}$ reveals an interesting trend: as the thermal stability increases, the duplexes are enthalpically destabilized. This effect, which is most pronounced in **III***, is completely compensated for by an increase in entropic stabilization, ultimately leading to an unchanged free energy of duplex formation. An example of a platinum-DNA adduct that shows a similar behavior is the *inter*strand GG cross-link formed by cisplatin. In this case, an increase in T_m accompanied by enthalpic destabilization and entropic stabilization was found [33]. Here, however, the duplex is thermodynamically destabilized (ΔG) due to the fact that an unfavorable ΔH is only partially compensated for by an increase in ΔS. A similar effect associated with a *decrease* in melting point has been established for the 1,2 *intra*stand cross-link [34]. An NMR-solution structure of the GG *inter*strand cross-link shows disruption of Watson-Crick hydrogen bonding at the binding site and altered stacking of the bases, resulting in a structure in which the complementary C bases become extrahelical [35]. Cross-link formation can be excluded as an explanation for the increase in T_m detected for the monoadduct of PT-ACRAMTU (e.g., from the MALDI-TOF data). Both effects, the loss of intramolecular stabilizing forces and the increase in disorder due to structural perturbations, are contributors to the change in thermodynamic stability of the cisplatin-modified duplexes. While the origin at the molecular level of the enthalpy-entropy compensation observed in **III*** remains to be further investigated, we speculate that PT-ACRAMTU may not cause major structural distortions, such as destacking and base-pair disruption.

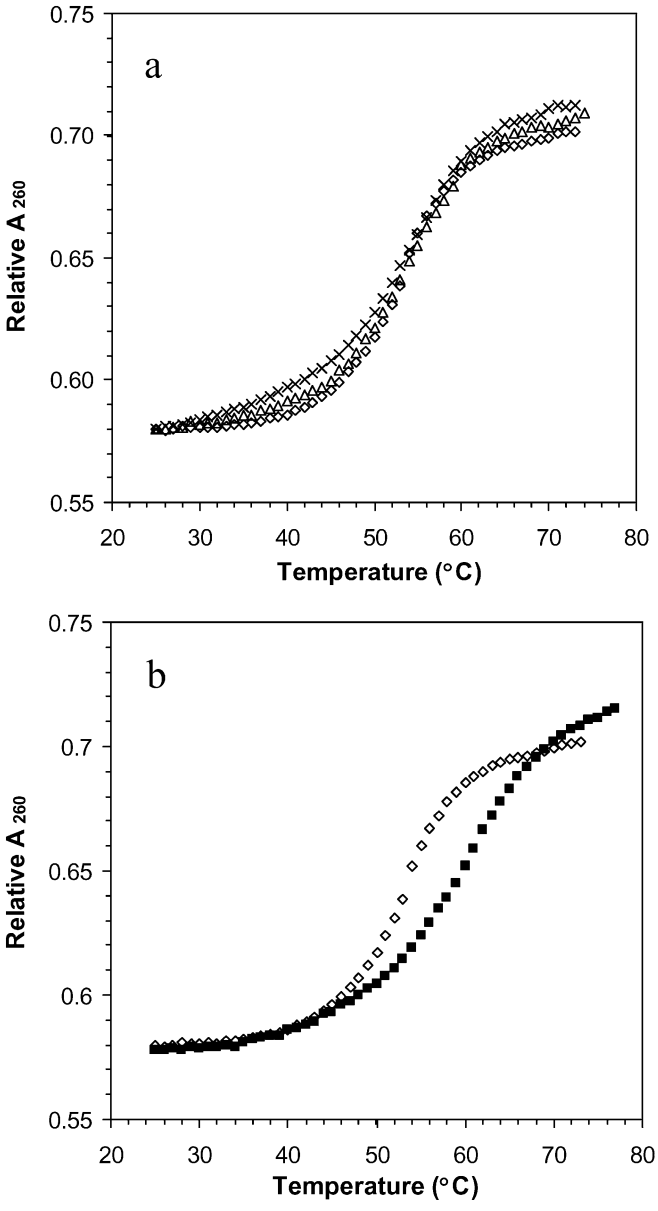

Fig. 5a, b UV-melting profiles monitored at 260 nm for the unmodified and modified sequences at a duplex concentration of 2.3 μM. **a** Normalized traces for **III** (*open diamonds*), **III**·ACRAMTU (*open triangles*), and **III**·3ACRAMTU (*crosses*). **b** normalized traces for **III** (*open diamonds*) and **III*** (*filled squares*)

Molecular modeling

To investigate the feasibility of the proposed coordinative-intercalative binding mode in **III*** (major-groove

Table 1 Thermal melting data and thermodynamic parameters for the unmodified and modified duplexes[a]

Duplex	T_m (°C)	ΔH_{vH} (kcal/mol)	ΔS_{vH} (cal/mol K)	$\Delta G_{vH,25}$[b] (kcal/mol)
III	52.8 ± 0.2	−67 ± 2	−206 ± 6	−4.5 ± 0.2
III·ACRAMTU	54.5 ± 0.2	−53 ± 2	−160 ± 6	−4.7 ± 0.2
III·3ACRAMTU	54.7 ± 0.2	−54 ± 2	−163 ± 6	−4.9 ± 0.2
III*	62.5 ± 0.6	−42 ± 2	−124 ± 6	−4.8 ± 0.3

[a]Derived from UV-melting profiles recorded at 260 nm for solutions containing 2.3 μM duplex. Thermodynamic data for duplex formation were calculated as described in the Materials and methods section and reflect the average of three measurements
[b]Extrapolated values assuming a temperature-independent transition enthalpy, ΔH_{vH}

binding of Pt to guanine-*N7* and insertion of the planar chromophore into the 5′-C6G19/G7C18 base step) and its impact on the conformation of the B-type duplex, a combined molecular-mechanics/molecular-dynamics study was performed. The parameterization of the AMBER force field used in this study took advantage of the knowledge of the crystal structure of dGuo*. Details of the modeling procedures and calculations are described in the Materials and methods section. A stereoview of the final energy-minimized model of **III*** is shown in Fig. 6, and selected base-pair and base-step parameters and torsionals for the modified duplex are summarized in Tables 2 and 3, respectively. The DNA retains its right-handed B-form with *anti* glycosidic torsion angles (χ), but the model shows adduct-induced perturbations at and beyond the platinated base pair and the site of intercalation. Some of the sugar puckers no longer adopt a C2′-*endo* conformation but have changed to conformations ranging from C1′-*exo* to C3′-*endo*, as indicated by the smaller pseudorotation angles (*P*). Intercalation of the acridine moiety causes significant distortions in the base pair adjacent to the platinum binding site (G7-*N7*): a buckle of 19.4° and a propeller twist of −29.8° are observed for C6G19. While the duplex is noticeably unwound at the central base step, as evidenced by the reduced twist angle (Ω) of 18.9° (and this effect extends into the neighboring base steps), the monoadduct produces only a small positive roll angle (ρ) of 9.9°, which does not lead to significant bending toward the major groove. The covalent G7-*N7* linkage produces close contacts between the thiourea linker and the walls of the major groove, which prevents the planar chromophore from penetrating deeply into the base stack (Fig. 7a). This is in contrast to the mode of intercalation of ACRAMTU, which allows a higher degree of overlap of the ligand and DNA-base-pair aromatic π-systems (Fig. 7b).

In summary, the model generated in this study demonstrates that the major groove of B-type DNA can accommodate the guanine-*N7* monoadduct of PT-ACRAMTU without suffering major destabilization. The partial-intercalation model of the chromophore supports the ICD and NMR data and previous DNA-unwinding experiments. Furthermore, the nondenaturing structural distortions of the helix at, and adjacent to, the adduct might explain the thermodynamic properties determined in the thermal melting experiments. Finally, the model does not appear to mimic or resemble solution and solid-state structures of severely bent duplex-DNA

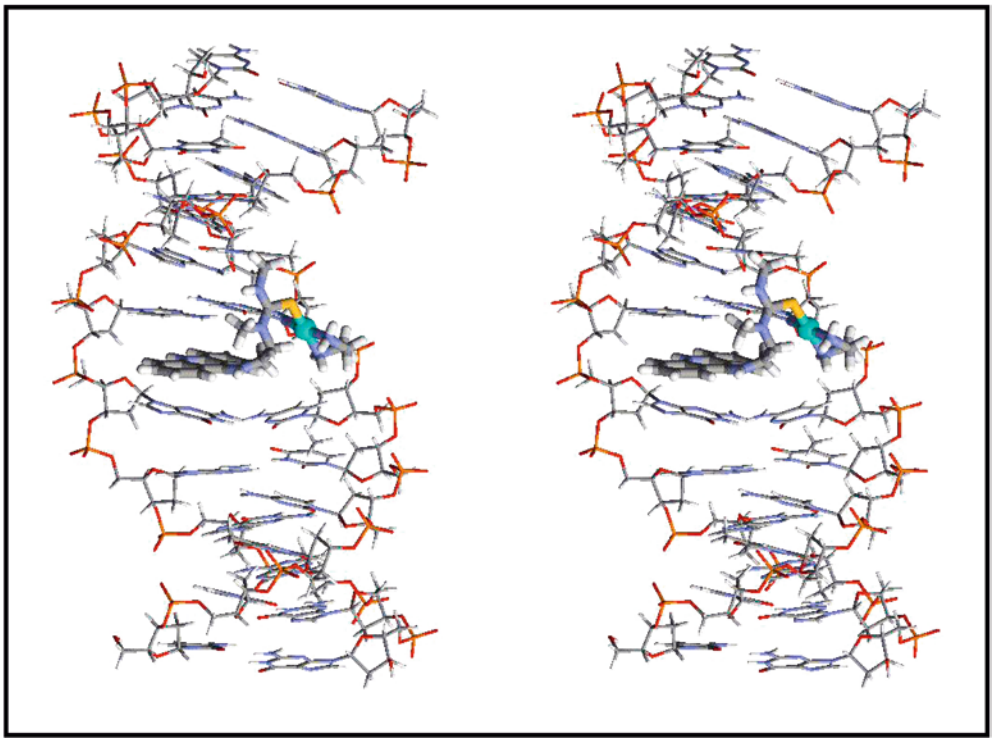

Fig. 6 Stereoview of the energy-minimized AMBER model of **III*** (view into the major groove)

Table 2 Selected DNA structural base-pair parameters calculated for the energy-minimized AMBER model of **III***[a]

Base pair	Buckle (κ) (°)	Opening (σ) (°)	Propeller twist (ω) (°)	P[b] (°)	Sugar pucker	χ[c] (°)
T5-A20	−5.4	−5.1	−14.0	30/92	C3′-endo/O4′-endo	−146/−158
C6-G19	**19.4**	0.9	**−29.8**	42/19	C4′-exo/C3′-endo	−138/−149
G7*-C18	−9.0	0.8	0.16	146/27	C2′-endo/C3′-endo	−117/−144
T8-A17	−0.1	−1.9	−13.7	137/37	C1′-exo/C4′-exo	−125/−148
C9-G16	−9.1	−2.8	−19.1	128/135	C1′-exo/C1′-exo	−123/−118

[a]Calculated with NAMOT
[b]Pseudorotation angle of the furanose, based on endocyclic torsion angles
[c]Glycosyl torsion angle (O4′-C1′-N1′-C2 for pyrimidines, O4′-C1′-N9-C4 for purines)

Table 3 Selected DNA structural base-step parameters calculated for the energy-minimized AMBER model of **III***[a]

Base step	Roll (ρ) (°)	Tilt (τ) (°)	Twist (Ω) (°)	Rise (D_z) (Å)
C4-G21/T5-A20	0.19	0.7	41.4	3.12
T5-A20/C6-G19	9.5	−9.0	27.0	3.30
C6-G19/G7*-C18	9.9	0.4	**18.9**	**6.14**
G7*-C18/T8-A17	0.8	−0.5	27.8	3.32
T8-A17/C9-G16	4.9	0.4	33.8	3.05

[a]Calculated with NAMOT

modified by the 1,2 *intra*strand cross-link [21, 22], the major adduct formed by cisplatin. NMR-solution studies of model duplexes containing dGuo* are currently underway to substantiate this notion.

Concluding remarks

A unique covalent-intercalative binding mode was established for the (potentially cytotoxic) major DNA adduct formed by PT-ACRAMTU, a new hybrid anticancer agent. The conjugate damages DNA in a way that appears to be distinctly different from the structural insult produced by its two constituents, ACRAMTU, the reversible minor-groove-directed intercalating agent, and the monofunctional platinum moiety. Conjugation of the two DNA-binding moieties leads to changes in duplex structure and stability that indicate synergistic action of the two binding modes. The coordinative-intercalative adduct of PT-ACRAMTU seems to incorporate itself seamlessly into the context of B-type DNA, unlike cisplatin, which distorts the duplex significantly through bending/base destacking (1,2 *intra*strand adduct) and disruption of interbase hydrogen bonding (1,2 *inter*strand adduct). These differences may lead to a type of drug action dissimilar to that of the clinical agents due to changed recognition of this adduct and its cellular processing and repair by enzymes. This supposition is supported by the promising biochemical and clinical properties of other nonclassical platinum-containing agents, such as multinuclear complexes and complexes exhibiting trans geometry [36]. Differences at the DNA–adduct level have been invoked as a crucial factor contributing to the distinct biological behavior of these compounds. A detailed NMR/MM/rMD study is currently underway using various model duplexes to determine the solution structure of the monoadduct of PT-ACRAMTU and its structural impact in duplex DNA.

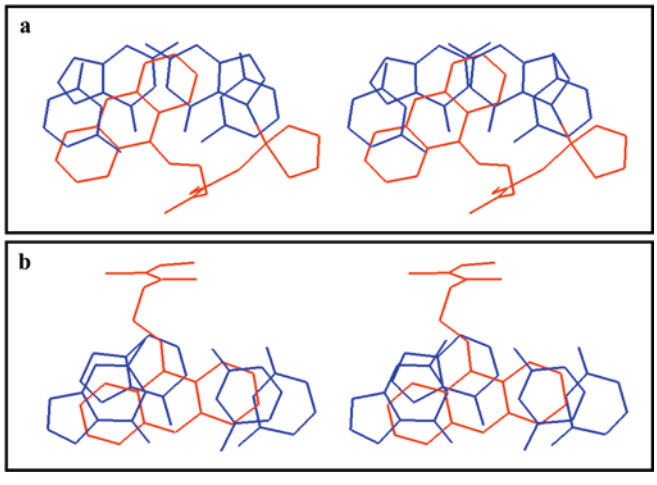

Fig. 7a, b Stereoviews along the helical axes of the intercalation sites of the acridine chromophores **a** in **III*** and **b** in d(GGAGCTCC)$_2$·(ACRAMTU)$_2$ (adopted from Ref. [6]). The nucleobases are depicted in *blue* and the (platinum-)acridine moieties in *red*

Acknowledgements This work was supported by a Research Project Grant from the National Institutes of Health/National Cancer Institute (R01 CA101880).

References

1. Sikora K, Advani S, Koroltchouk V, Magrath I, Levy L, Pinedo H, Schwartsmann G, Tattersall M, Yan S (1999) Ann Oncol 10:385–390
2. Martins ET, Baruah H, Kramarczyk J, Saluta G, Day CS, Kucera GL, Bierbach U (2001) J Med Chem 44:4492–4496
3. Baruah H, Rector CL, Monnier SM, Bierbach U (2002) Biochem Pharmacol 64:191–200
4. Gelasco A, Lippard SJ (1999) In: Clarke MJ, Sadler PJ (eds) Topics in biological inorganic chemistry, vol. I. Springer, Berlin Heidelberg New York, pp 1–43
5. Bowler BE, Lippard SJ (1986) Biochemistry 25:3031–3038

6. Holmes RJ, McKeage MJ, Murray V, Denny WA, McFadyen WD (2001) J Inorg Biochem 85:209–217
7. Perrin LC, Prenzler PD, Cullinane C, Phillips DR, Denny WA, McFadyen WD (2000) J Inorg Biochem 81:111–117
8. Gibson D, Mansur N, Gean KF (1995) J Inorg Biochem 58:79–88
9. Gean KF, Ben-Shoshan R, Ramu A, Ringel I, Katzhendler J, Gibson D (1991) Eur J Med Chem 26:593–598
10. Cullinane C, Wickham G, McFadyen WD, Denny WA, Palme BD, Phillips DR (1993) Nucleic Acids Res 21:393–400
11. Temple MD, McFadyen WD, Holmes RJ, Denny WA, Murray V (2000) Biochemistry 39:5593–5599
12. Barry CG, Baruah H, Bierbach U (2003) J Am Chem Soc 125:9629–9637
13. Baruah H, Bierbach U (2003) Nucleic Acids Res 31:4138–4146
14. Jenkins TC (1997) In: Fox KR (ed) DNA-drug interaction protocols. Humana, Totowa, NJ, pp 195–218
15. Marky LA, Breslauer KJ (1987) Biopolymers 26:1601–1620
16. Kozelka J, Archer S, Petsko GA, Lippard SJ (1987) Biopolymers 26:1245–1271
17. Hambley TW (1991) Inorg Chem 30:937–942
18. Yao S, Plastaras JP, Marzilli LG (1994) Inorg Chem 33:6061–6077
19. Bierbach U, Farrell N (1997) Inorg Chem 36:3657–3665
20. Lemaire M-A, Schwartz A, Rahmouni AR, Leng M (1991) Proc Natl Acad Sci USA 88:1982–1985
21. Takahara PM, Frederick CA, Lippard SJ (1996) J Am Chem Soc 118:12310–12321
22. Gelasco A, Lippard SJ (1998) Biochemistry 37:9230–9239
23. Brabec V, Kleinwächter V, Butour J-L, Johnson NP (1990) Biophys Chem 35:129–141
24. Wirth M, Buchardt O, Koch T, Nielsen PE, Nordén B (1988) J Am Chem Soc 110:932–939
25. Kim H-K, Kim J-M, Kim S-K, Rodger A, Nordén B (1996) Biochemistry 35:1187–1194
26. Giménez-Arnau E, Missailidis S, Stevens MFG (1998) Anti-Cancer Drug Design 13:431–451
27. Fornasiero D, Kurucsev T (1985) Biophys Chem 23:31–37
28. Gray DM, Ratliff RL, Vaughan MR (1992) Methods Enzymol 211:389–406
29. Schipper PE, Nordén B, Tjerneld F (1980) Chem Phys Lett 70:17–21
30. Wilson WD, Li Y, Veal JM (1992) In: Hurley LH (ed) Advances in DNA sequence specific agents. JAI, New York, pp 89–165
31. SantaLucia Jr J (1998) Proc Natl Acad Sci USA 95:1460–1465
32. Peleg-Shulman T, Katzhendler J, Gibson D (2000) J Inorg Biochem 81:313–323
33. Hofr C, Brabec V (2001) J Biol Chem 276:9655–9661
34. Poklar N, Pilch DS, Lippard SJ, Redding EA, Dunham SU, Breslauer KJ (1996) Proc Natl Acad Sci USA 93:7606–7611
35. Huang H, Zhu L, Reid BR, Drobny GP, Hopkins PB (1995) Science 270:1842–1845
36. Zhang CX, Lippard SJ (2003) Curr Opin Chem Biol 7:481–489